Intake O2 Concentration Estimation in a Turbocharged Diesel Engine through NOE

Intake O_2 Concentration Estimation in a Turbocharged Diesel Engine through NOE

Loris Ventura[1*] and Stefano A. Malan[2]
[1]Department of Energy, Politecnico di Torino, Corso Duca degli Abruzzi 24, 10129, Torino, Italy (loris.ventura@polito.it)
*Corresponding author
[2]Department of Electronics and Telecommunications, Politecnico di Torino, Corso Duca degli Abruzzi 24, 1029, Torino, Italy (stefano.malan@polito.it)

Abstract

Diesel engines with their embedded control systems are becoming increasingly complex as the emission regulations tighten, especially concerning NO_x pollutants. The combustion and emission formation processes are closely correlated to the intake manifold O_2 concentration. Consequently, the performance of the engine controllers can be improved if a model-based or sensor-based estimation of the O_2 concentration is available. The paper addresses the modeling of the O_2 concentration in a turbocharged diesel engine. Dynamic models, compared to generally employed steady state maps, capture the dynamic effects occurring over transients, when the major deviations from the stationary maps are found. Dynamic models positively affect the control system making it more effective and, exploiting information coming from sensors, they provide a more robust prediction performance. Firstly, a Nonlinear Output Error model (NOE), with simulation focus, fed with four inputs is presented. The considered nonlinear function set is the one of neural networks. The inputs are engine BMEP, engine RPM and EGR and VGT valves position. Two distinct datasets are used for training and validation of the NOE model. These sets are generated using GT-Power simulation software implementing a fine model of the engine, previously validated on experimental measurements taken on the real engine. Besides the transient validation, the NOE model was tested against GT-Power outputs on step tests involving the EGR and VGT actuators. At last the network output is compared with an O_2 steady state map over a transient in normal and faulty conditions. The performance of the model is satisfactory in both conditions. Secondly, the potential benefits of installing an O_2 sensor in the intake manifold is presented: a Nonlinear Auto-Regressive with eXogenous input (NARX) model is considered and compared to the previously investigated NOE. The results prove that, exploiting the output coming from the O_2 sensor, the model prediction capability significantly improves.

Introduction

As environmental awareness grows, emissions limit legislation becomes increasingly more severe. To comply with these regulations in the automotive field a wide range of technological solutions have been developed. Exhaust Gas Recirculation (EGR) and Variable Geometry Turbochargers (VGTs) [1], high-pressure common rail injection systems [2-6], advanced combustion control and innovative combustion concepts [7-8] represent some of these technologies. Among these solutions, the development of model-based advanced controllers is becoming more and more important.

It is generally agreed that diesel engines will remain the main propulsion system for heavy-duty vehicles at least for the following 20-30 years. Consequently, the research effort in this field is moving toward the development of control strategies that take directly into account the pollutants.

The air-path control system has to ensure that a fresh air-exhaust gases mixture of the desired composition and with sufficient oxygen content enters into the cylinders. At the same time the combustion control system has to determine the appropriate fuel quantity and injection timing for the given load request and cylinder content. The correct functioning of these two control systems allows the after-treatment controller to work properly reducing the pollutants to the regulated standards. In all these control systems the oxygen concentration in the intake manifold plays a key role in their operation.

In this work the modeling of the intake O_2 concentration is addressed. The choice of this variable is motivated by its strict linear correlation with NO_x pollutant emissions. For a complete treatise refer to [9]. Therefore, the knowledge of the intake O_2 concentration is fundamental to ensure the correct engine functioning and low engine-out NO_x emissions. Consequently, the performance of the main engine controllers can be improved significantly if a model-based or sensor-based estimation of the intake O_2 concentration is available in the ECU. The objective of this paper is the modeling of the intake O_2 concentration through neural networks.

In the literature the intake O_2 concentration is generally modeled through Mean Value Engine Models (MVEM) of the filling and emptying type based on energy and mass equations. An example of this kind of models can be found in [10]. In [11] the stability and observability properties of a MVEM model for the estimation of the intake oxygen concentration are discussed. Paper [12] proposes a linear parameter varying model while in [13] extended Kalman filter for the estimation of the intake O_2 concentration is adopted. In [14] the existing transport delay between exhaust and intake manifold has been considered. Another approach is the use of multiple linear black-box models. This method is applied in [9] exploiting the systematic procedure described in [15].

In the following of the paper, Section *Problem Definition* presents the characteristics of the engine considered in this work and the training and validation datasets. Training and validation results are presented in Section *RNN Performances Results* together with actuators step tests, comparison with steady state map and sensor-based prediction. Conclusions are given in the last Section.

Problem Definition

The intake manifold O_2 concentration can be retrieved by means of different approaches.

One of the most generally used approach is through steady state maps, that are function of engine RPM and BMEP as in engine practice is convenient to refer quantities to the engine working point. Starting from the engine calibration process, set points are defined from steady state measurements and stored as a function of RPM and BMEP.

Another possibility to accomplish the intake O_2 computation is exploiting EGR rate X_r and relative air-to-fuel ratio λ:

$$O_2 = a_1 \frac{X_r}{\lambda} + a_2 \quad (1)$$

Using the linear relation described in Equation (1), where a_1 and a_2 are two scalar coefficients, it is possible to estimate in real time the O_2 value. A complete description of this last method and the use of steady state maps is given in [16]. It must be pointed out that both these approaches are stationary methods that cannot precisely describe the transient behavior of the intake O_2 concentration.

One more possibility is the direct measurement installing an O_2 sensor in the intake manifold. The drawback of this solution is the increased engine setup complexity and the necessity to suitably process and filter the acquired signal.

Here it has been chosen to identify a dynamic nonlinear model to simulate and predict the intake O_2 concentration. This model is suitable for implementation within an air-path or combustion control system or for fault and diagnostic purposes. The O_2 model overcomes the limitation of steady state maps or linear stationary models, as the one in Equation (1), being dynamic and able to account for multiple inputs, thus increasing the robustness of the system. The model has been developed for simulation purposes, which is for use without an O_2 sensor. Simulation means to use the model for an infinite step ahead output prediction without exploiting any information from the actual output. This has been chosen in order not to increase the complexity of the engine setup. Nonetheless, a model, with a different suitable structure, can also exploit the information coming from a sensor for one step ahead predictions. In this situation the predicted output is computed using the information from the actual output at the previous time steps.

Table 1. FPT F1C Engine Main Specifications.

Engine type	FPT F1C EURO VI diesel engine
Number of cylinders	4
Displacement	2998 cc
Bore x stroke	95.8 x 104 mm
Rod length	160 mm
Compression ratio	17.5 : 1
Valves per cylinder	4
Turbocharger	VGT type
Fuel injection system	High pressure common rail

Engine

The engine considered in this work is an FPT F1C 3-litre EURO VI diesel modeled in GT-Power environment. It is endowed with short route EGR, VGT, Exhaust flap, Intercooler and EGR cooler. The main specifications of the engine are reported in Table 1 while the engine layout is shown in Fig.1.

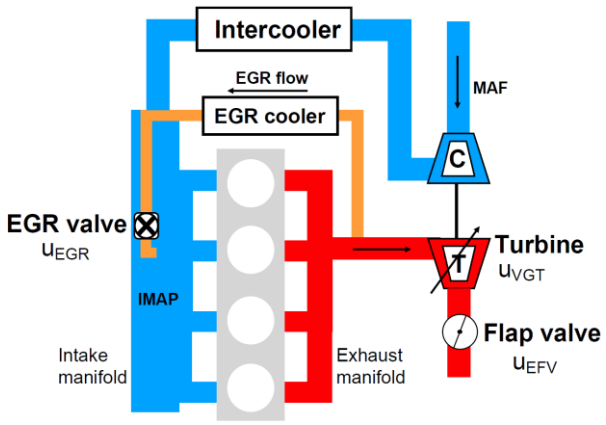

Figure 1. FPT F1C Engine layout.

Recurrent Neural Network

The nonlinear dynamic model considered in this work to compute the intake O_2 concentration is obtained from the neural networks nonlinear function set [17].

Four inputs are provided to the network to estimate the intake manifold O_2 concentration. They are the opening positions u_{EGR} *and* u_{VGT} of EGR and VGT valves, engine Brake Mean Effective Pressure (BMEP), u_{BMEP}, and speed (RPM), u_{RPM}. The chosen regressor $\varphi(t)$ is shown in Equation (2)

$$\begin{aligned}\varphi(t) = \big[&\hat{y}(t-1)\cdots\hat{y}(t-n_f),\\ &u_{EGR}(t-n_k)\cdots u_{EGR}(t-n_k-n_b-1),\\ &u_{VGT}(t-n_k)\cdots u_{VGT}(t-n_k-n_b-1),\\ &u_{BMEP}(t-n_k)\cdots u_{BMEP}(t-n_k-n_b-1),\\ &u_{RPM}(t-n_k)\cdots u_{RPM}(t-n_k-n_b-1)\big]\end{aligned} \quad (2)$$

where $\hat{y}$ is the predicted output, that is to say the predicted O_2 concentration, n_f and n_b represent the numbers of signal past samples used as input to the network and n_k the input delay. The output is expressed by the predictor (3)

$$\hat{y}(t|\theta) = g(\varphi(t), \theta) \quad (3)$$

where θ is a vector containing the weights and biases and g is the non-linear function realized by the neural network. The neural network uses hyperbolic tangent neurons in the hidden layer and linear functions in the output layer.

The regressor in Equation 2 corresponds to a Nonlinear Output Error (NOE) model [18]. As the input layer consist of past predictions by including a feedback path from the output layer this model is equivalent to a Recurrent Neural Network (RNN).

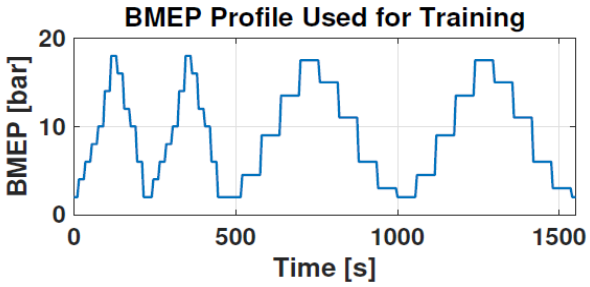

(a)

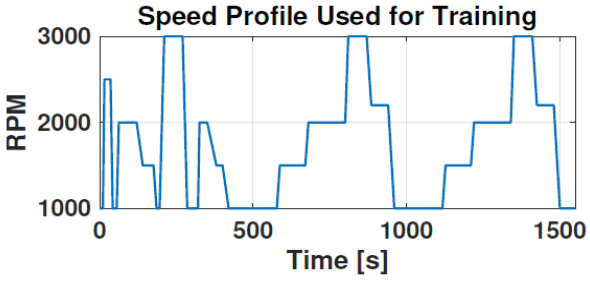

(b)

Figure 2. a) Engine BMEP profile used for training. b) Engine speed profile used for training.

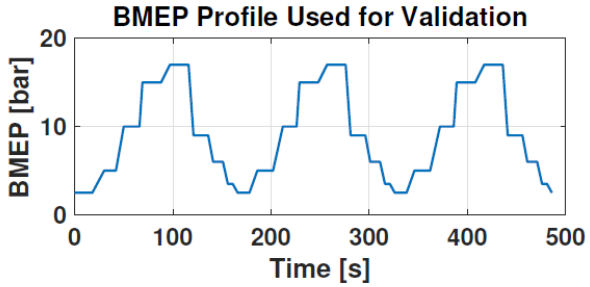

(a)

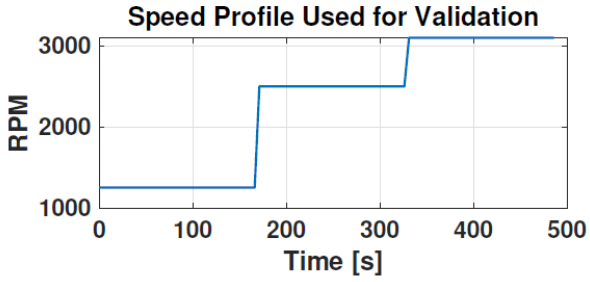

(b)

Figure 3. a) Engine BMEP profile used for validation. b) Engine speed profile used for validation.

In the Output Error (OE) model family, there is no attempt to model the noise characteristic that is assumed to be white. It directly affects the output, acting on top of it, without being filtered by a transfer function. The OE predictions are solely based on inputs, there is no feedback from measurements. Since the predictor solely focuses on the deterministic portion (no noise characteristic involved), this structure has an advantage under open-loop conditions. Technically, this open-loop condition is known as "infinite step ahead prediction" or "simulation" [18].

On the data side, two separate datasets were used for training and validation purposes, that are the two needed procedural steps to obtain an effective model. These two sets of numerical data were generated using the GT-Power engine model. The commands of the valves were constituted by random amplitude signals while ramp profiles were used for engine BMEP and RPM both for training and validation purposes (Fig.2 and 3). These data were preliminarily scaled and normalized in order to obtain a dataset characterized by zero mean and variance equal to 1. This allows to reduce numerical errors and to have faster convergence of the training algorithm. The training was performed using the Levenberg-Marquardt method [19] and it was carried out in MATLAB environment through NNSYSID toolbox [20].

To further extend the validation tests, investigation was carried forward to check if the network was able to reproduce the effect of a single actuator. Then each one of the two actuators was commanded with a wave with random amplitude and keeping the other actuator position fixed.

RNN Performances Results

This section presents the simulation results of the training and validation steps of the estimated network, actuators step test results and comparison between simulation and prediction aims.

Training and Validation

The NOE model has been chosen among others because it has shown the best results. The network topology has been chosen among networks up to 5 neurons in the hidden layer and varying the regressor parameters n_f, n_k and n_b from 1 to 4. Then the network that has shown the best performance in terms of Root Mean Square Error (RMSE) and computational cost has been chosen.

The selected network, which is shown in Fig.4a, is characterized by 2 hidden neurons and one-neuron output layer. The 5 neurons in the input layer correspond to the 4 physical inputs plus the feedback of the past value of the simulated output, as highlighted in Fig.4b. The corresponding parameters are $n_f = 1$, $n_k = 1$, and $n_b = 1$. Training results are shown in Fig.5 and 6 respectively. On the y axis the scaled value of the intake O_2 concentration is reported. It expresses only the variation of the oxygen with respect to the average value and for this reason it is indicated with ΔO_2.

From Fig.5 it is visible that the network is able to reproduce with good accuracy the training dataset. Moreover, as can be seen in Fig.6, the major deviations of model data from experimental data, that is the deviation of the blue points from the red line, coincide with the lower peaks of Fig.5 at time instants t=0s, t=200s and just after t=500s. The RMSE on this simulation is 0.41. Networks that have shown better training results happened to be ineffective in the validation process.

On the validation side, by looking at Fig.7a, some differences between validation data and model output are noticed. The peak at time t=225s is due to aggressive opening of the EGR valve and closing of the VGT one at high engine load. This aggressive response of both actuators determines a reduction in the intake O_2 concentration that the model is not able to follow. This also occurs, but with smaller amplitude, from time t=410s to time t=440s. However, the overall performance of the network is acceptable because hardly the actuators will move in such a way in real driving conditions.

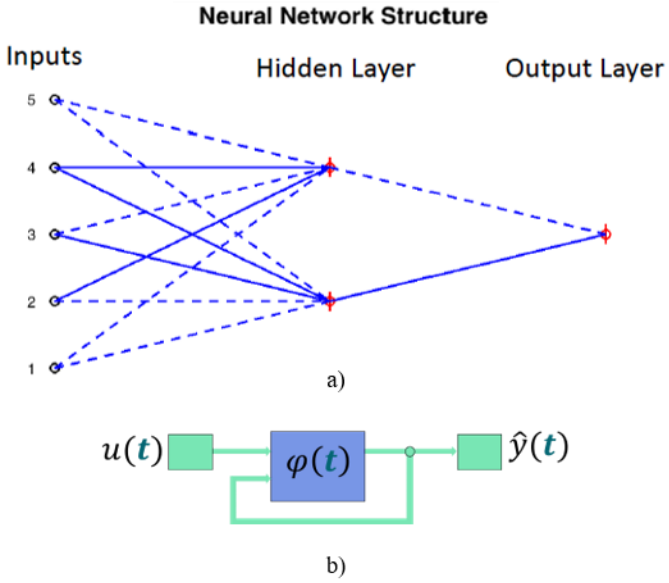

Figure 4. a) 1112 NOE layout. b) Intrinsic feedback from simulated output.

Figure 5. Neural network training results.

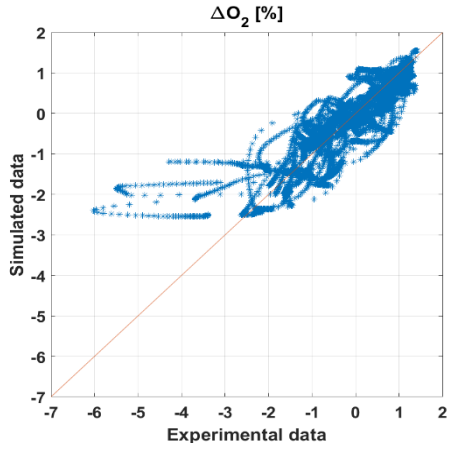

Figure 6. Simulated vs. experimental values of the intake O_2 concentration.

The relative error on the validation dataset is shown in Fig.7b. It is generally within the ±5% range (dotted gray lines) apart from the peaks explained before exceeding the 10% (black dashed line). The RMSE on the validation simulation is 0.76

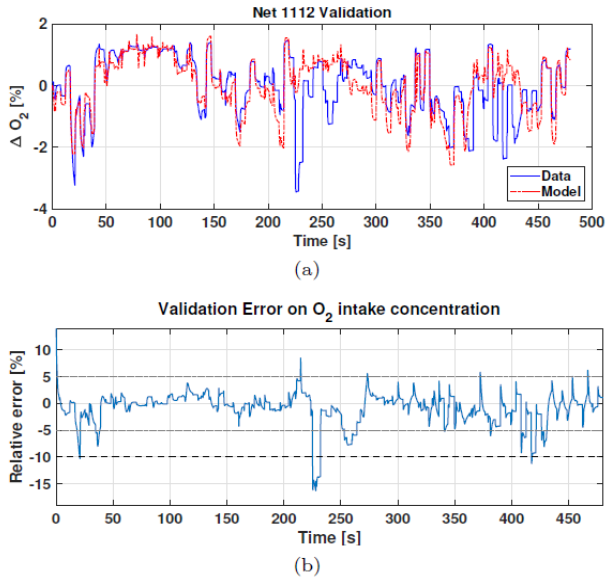

Figure 7. a) Network validation simulation. b) Network validation error.

Step Tests

Figure 8a shows the simulation of an EGR valve step. Note that in this and following plots the total value of intake O_2 concentration is shown, not only the variation with respect to the mean value, as in the previous ones. The model shows a slower and smaller amplitude response compared to the GT-Power one. In Fig.8b the error on the EGR step simulation in shown. It reaches the 2% on the upper peak corresponding to an overshoot occurring when the EGR valve is closed. On the EGR valve step the RMSE is 0.21. Figure 9a reports the results of the simulation of a VGT step. The model well approximates the response showing a first order behavior thus neglecting overshoots. However, an offset between the two responses is clearly visible. In Fig.9b the error of the network on the VGT step is reported. It is always positive and lower than the 2%. The resulting RMSE is 0.24. Both simulations present differences from the respective GT-Power data. Still, the results are acceptable since the error is lower than the 5%.

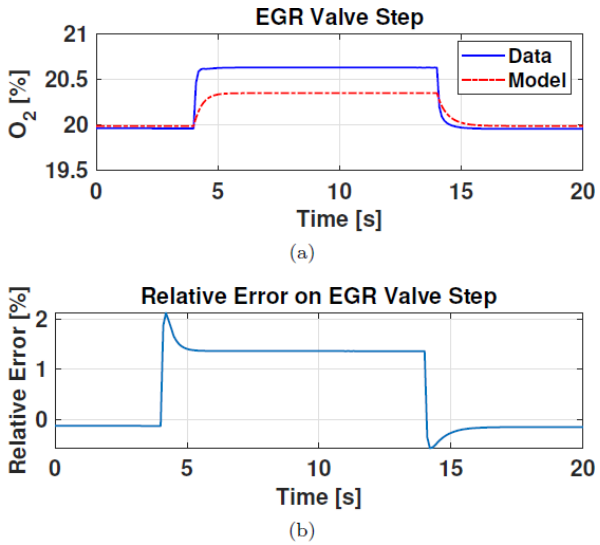

Figure 8. a) Gt-Power and network simulation for an EGR step input. b) Error on the EGR step simulation.

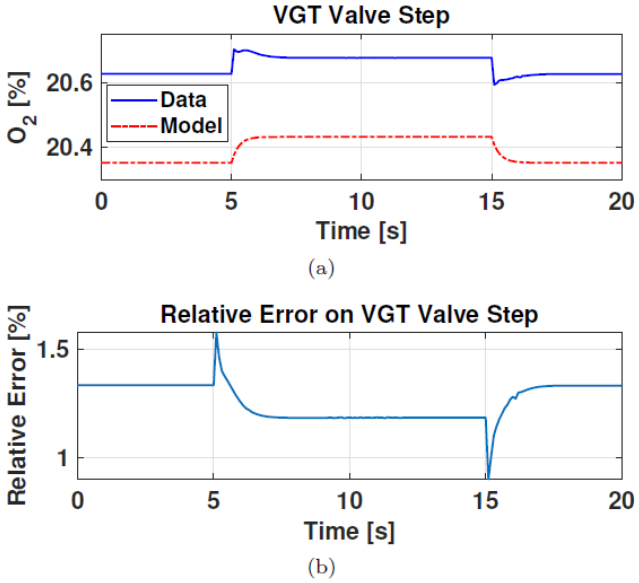

Figure 9. a) Gt-Power and network simulation for a VGT step input. b) Error on the VGT step simulation.

NOE and Steady State Map Comparison

Figure 10 illustrates the comparison between the intake O_2 concentration estimated by the selected network and the one estimated by means of a steady state map, in which the intake O_2 concentration is stored as a function of engine speed and load on the basis of the steady state working points. The limitation of a steady state map, compared to a dynamic model, is clear. The map does not contain information on the dynamics of the system, it only operates by interpolating the stored values. For this reason, its lack of performance especially during transient operations can produce undesired effects. However, thanks to their simplicity maps are widely used on production engines.

NOE and Steady State Map Comparison

Figure 10 illustrates the comparison between the intake O_2 concentration estimated by the selected network and the one estimated by means of a steady state map, in which the intake O_2 concentration is stored as a function of engine speed and load on the basis of the steady state working points. The limitation of a steady state map, compared to a dynamic model, is clear. The map does not contain information on the dynamics of the system, it only operates by interpolating the stored values. For this reason, its lack of performance especially during transient operations can produce undesired effects. However, thanks to their simplicity maps are widely used on production engines.

The simulation is shown in Fig.10a with the blue continuous line representing GT-Power data, the red dashed-dotted line representing the network and the black dashed line representing the O_2 map. The network response well approximates the GT-Power data while the map underestimates the oxygen concentration. The error trends are shown in Fig.10b. Here the error of the network is contained in the ±5% region represented by the gray dotted lines with only the peaks exceeding it. By looking at the error of the steady state map it is visible that it is generally higher than the error of the network.

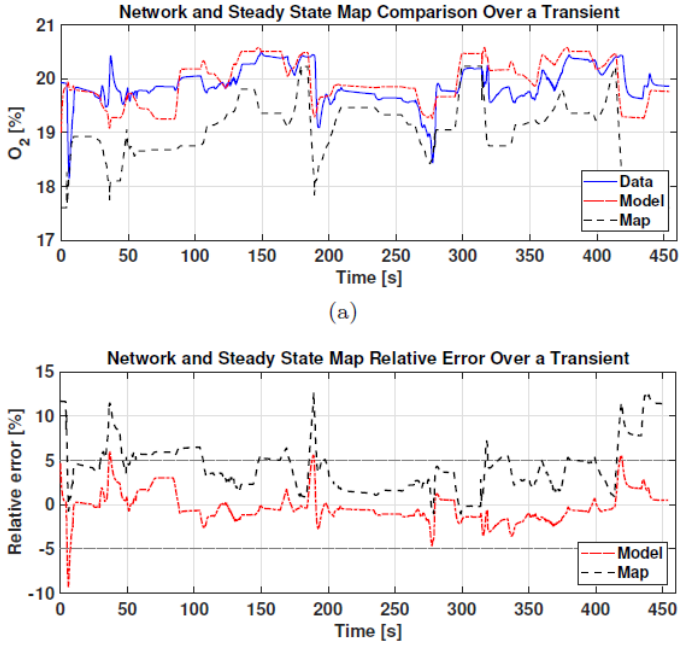

Figure 10 a) Neural network and steady state map output comparison over a transient. b) Error comparison between estimated network and steady state map.

The simulation is shown in Fig.10a with the blue continuous line representing GT-Power data, the red dashed-dotted line representing the network and the black dashed line representing the O_2 map. The network response well approximates the GT-Power data while the map underestimates the oxygen concentration. The error trends are shown in Fig.10b. Here the error of the network is contained in the ±5% region represented by the gray dotted lines with only the peaks exceeding it. By looking at the error of the steady state map it is visible that it is generally higher than the error of the network.

In addition to this test at normal working condition a simulation replicating it but in faulty condition with partially obstructed EGR valve has been performed (Fig.11). The obstruction has been modeled in GT-Power reducing the discharge coefficient of the EGR valve. Figure 11a illustrates the simulation of a transient performed with partially obstructed EGR valve. The GT-Power track, blue continuous line, is shifted upward compared to Fig.10a. This is due to the lower EGR rate caused by the obstruction. The other two tracks of the network, red dashed-dotted line, and the map, black dashed line, are the same as in Fig. 10a since no information is provided to them about the obstruction.

The error on this simulation is shown in Fig.11b. In this scenario the performance of the network remains good with the error still being contained in the ±5% range. On the contrary the map error increases compared to the normal condition of Fig.10b.

Exploiting the feedback from an O_2 sensor it is possible to use the network as a reference of the correct engine functioning. If the difference between the sensor measurement and the network output exceeds a given threshold, say 20% for example, the probability of that the engine is not running in safe conditions will be high. The steady state map presents an error that is higher than the network one, so the possibility of incurring in a false positive is higher.

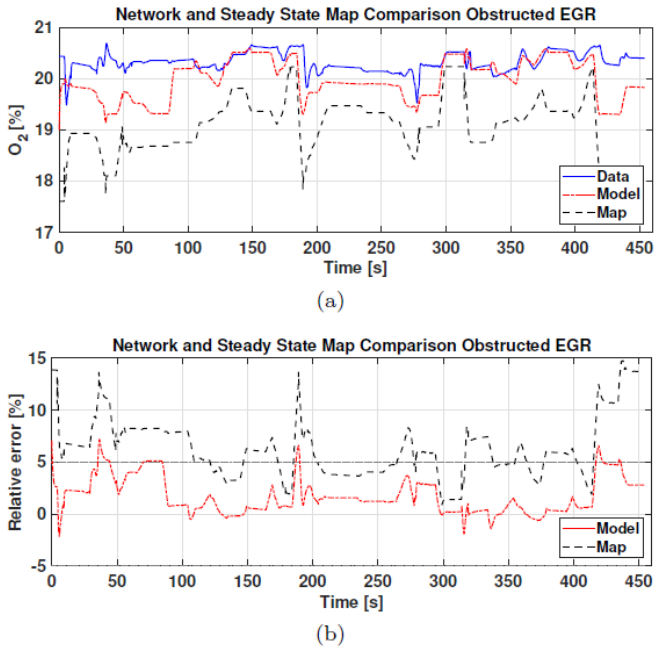

Figure 11 a) Neural network and steady state map output comparison over a transient with obstructed EGR. b) Error comparison between estimated network and steady state map.

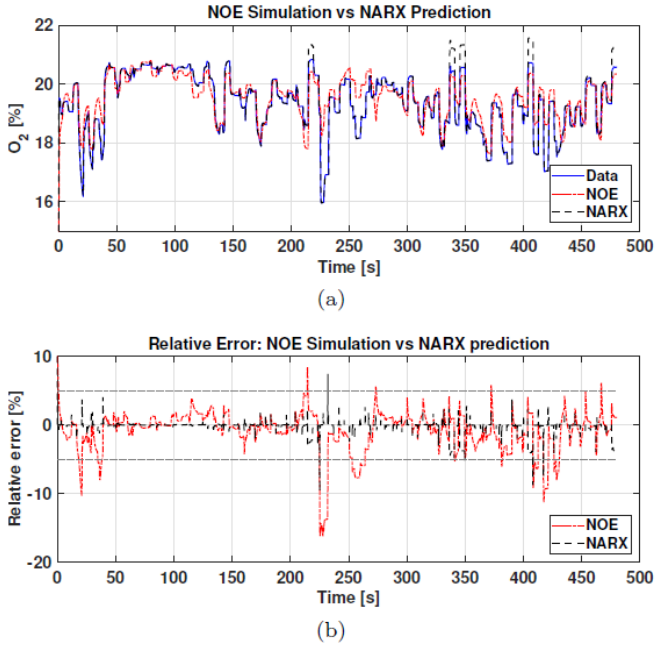

Figure 12 a) NOE simulation vs NARX 1-step ahead prediction comparison over the validation dataset. b) Error comparison between NOE and NARX.

NOE simulation vs NARX prediction

As final experiment the estimated NOE has been compared with a NARX of the same topology (n_a=n_b=n_k=1, with 2-neurons hidden layer and 1-neuron output layer). This was done to check the potential benefits of installing an O_2 sensor in the intake manifold. Indeed the NARX model can exploit the measurements coming from the sensor to predict the future values of the estimated output. NARX models thus do not use feedback of their own predictions, substituting it with the sensor measurement; contrary to NOE models that use feedback. In other words, in NARX models the next value of the dependent output signal *y(t)* is regressed on previous values of the true output signal (instead of the estimated one, as in NOE models) and previous values of an independent (exogenous) input signal. In NARX models the predictor is exactly as in Equation (3), while the regressor now is

$$\begin{aligned}\varphi(t) = [&y(t-1)\cdots y(t-n_a),\\ &u_{EGR}(t-n_k)\cdots u_{EGR}(t-n_k-n_b-1),\\ &u_{VGT}(t-n_k)\cdots u_{VGT}(t-n_k-n_b-1),\\ &u_{BMEP}(t-n_k)\cdots u_{BMEP}(t-n_k-n_b-1),\\ &u_{RPM}(t-n_k)\cdots u_{RPM}(t-n_k-n_b-1)]\end{aligned} \quad (4)$$

where *y(·)* represents the past samples of the sensor measured signal, n_a represents the numbers of signals past samples used as input to the network. The other parameters and signals are as in Equation (2).

The exploitation of a sensor results in a more accurate model input. Furthermore, in the ARX model family the white noise (disturbance) is filtered by the system dynamics instead of acting directly on the output. This means that in ARX models the disturbances are part of the system dynamics.

Figure 12a shows the result of this comparison over the validation dataset. GT-power data are represented with the blue continuous line while NOE simulation is in red dashed-dotted line and the NARX prediction is in black dashed line. The NARX prediction differs from the GT-Power data only on some of the higher peaks. By looking at the error reported in Fig.12b, it can be noted that the NARX one step ahead prediction is very accurate expressing a smaller error than the NOE simulation.

This result states that the installation of an O_2 sensor in the intake manifold allows the use of different families of models and that the prediction ability can be greatly enhanced by the direct measurement of this signal.

Conclusions

The paper addressed the modeling of the intake O_2 concentration in a diesel engine. For this purpose, a neural network model is used instead of a traditional map-based approach. Among the different model classes and orders a first order NOE with 2-neurons hidden layer has shown the best performance. It has been validated over a transient dataset and tested over the single actuator variations. Then a comparison with the steady state map has been presented in normal and faulty conditions with obstructed EGR. The network has shown acceptable performance showing an error contained in the ± 5% range. Over transient conditions the prediction of the intake O_2 concentration improved significantly compared to steady state maps. If the measurement of the intake O_2 concentration is available, the NOE network could become a reference model for correct engine functioning and could be used for fault detection.

The use of neural network allows to increase the potential of model-based air-path control techniques due to their fast execution speed and low computational cost. Furthermore a precise intake O_2 concentration can be exploited from other engine controls improving the overall performance of the engine

To improve the performance of the model the training test will be re-designed avoiding undesired actuators combination. A further improvement can be obtained enlarging the test including single input step actuation over multiple engine points in a Design of Experiment (DOE) fashion. Furthermore, the adoption of an O_2 sensor can be considered to increase the accuracy even more as shown in Subsection *NOE simulation vs NARX prediction*.

References

1. Baratta, M., Finesso, R., Misul, D., and Spessa, E., "Comparison between Internal and External EGR Performance on a Heavy Duty Diesel Engine by Means of a Refined 1D Fluid-Dynamic Engine Model", SAE Int. J. Engines 8(5):1977-1992, 2015,.
2. Ferrari, A., Mittica, A., Pizzo, P. et al. "PID Controller Modelling and Optimization in Cr Systems with Standard and Reduced Accumulators". Int. J. Automot. Technol. 19, 771–781, 2018, doi:10.1007/s12239-018-0074-4
3. Ferrari, A., Mittica, A., Pizzo, P., Wu, X., and Zhou, H. (October 3, 2017). "New Methodology for the Identification of the Leakage Paths and Guidelines for the Design of Common Rail Injectors With Reduced Leakage". ASME. J. Eng. Gas Turbines Power. February 2018; 140(2): 022801. doi:10.1115/1.4037862.
4. Ferrari, A., Mittica, A., Paolicelli, F., and Pizzo, P., "Hydraulic characterization of solenoid-actuated injectors for diesel engine common rail systems", Energy Procedia, 101, 878 – 885, ATI 2016 - 71st Conf. of the Italian Thermal Machines Engineering Association, 2016, doi:10.1016/j.egypro.2016.11.111.
5. Catania, A., Ferrari, A., Mittica, A., and Spessa, E., "Common Rail without Accumulator: Development, Theoretical-Experimental Analysis and Performance Enhancement at DI-HCCI Level of a New Generation FIS", SAE Technical Paper 2007-01-1258, 2007, doi:10.4271/2007-01-1258.
6. Catania, A., Ferrari, A., and Mittica, A., "High-Pressure Rotary Pump Performance in Multi-Jet Common Rail Systems", Proceedings of the ASME 8th Biennial Conference on Engineering Systems Design and Analysis, Volume 4: Fatigue and Fracture, Heat Transfer, Internal Combustion Engines, Manufacturing, and Technology and Society, Torino, Italy. July 4–7, 2006. pp. 557-565. ASME, doi:10.1115/ESDA2006-95590.
7. Finesso, R.; Hardy, G., Mancarella, A., Marello, O., Mittica, A., Spessa, E., "Real-Time Simulation of Torque and Nitrogen Oxide Emissions in an 11.0 L Heavy-Duty Diesel Engine for Model-Based Combustion Control", Energies 12, no. 3: 460, 2019, doi:10.3390/en12030460.
8. D'Ambrosio, S., Gaia, F., Iemmolo, D., Mancarella, A. et al., "Performance and Emission Comparison between a Conventional Euro VI Diesel Engine and an Optimized PCCI Version and Effect of EGR Cooler Fouling on PCCI Combustion", SAE Technical Paper 2018-01-0221, 2018, doi:10.4271/2018-01-0221.
9. Ventura, L., Finesso, R., Malan, S.A., d'Ambrosio, S., and Manelli, A, "Model-based design of closed loop controllers of the air-path in a heavy duty diesel engine", 74th Congresso Nazionale ATI, AIP, Conference Proceedings, 2019, doi:10.1063/1.5138885.
10. Arsie, I., Cricchio, A., Pianese, C., and De Cesare, M., "Real-Time Estimation of Intake O2 Concentration in Turbocharged Common-Rail Diesel Engines", SAE Int. J. Engines 6(1):237-245, 2013, doi:10.4271/2013-01-0343.
11. Diop, Sette, P. E. Moraal, I. A. Kolmanovsky and M. J. van Nieuwstadt, "Intake oxygen concentration estimation for DI diesel engines", Proceedings of the 1999 IEEE International Conference on Control Applications (Cat. No.99CH36328) 1 (1999): 852-857 vol. 1, doi:10.1109/CCA.1999.807777.
12. Alberer, D. and del Re, L., "Fast Oxygen Based Transient Diesel Engine Operation", SAE Int. J. Engines 2(1):405-413, 2009, doi:10.4271/2009-01-0622.
13. Min, K., Shin, J., Jung, D., Han, M., and Sunwoo, M., "Estimation of Intake Oxygen Concentration Using a Dynamic Correction State With Extended Kalman Filter for Light-Duty Diesel Engines". ASME. J. Dyn. Sys., Meas., Control. January 2018; 140(1): 011013, doi:10.1115/1.4037390.
14. Meyer, J., Midlam-Mohler, S., and Yurkovich, S., "In-cylinder oxygen concentration estimation for diesel engines via transport delay modeling", Proceedings of the 2011 American Control Conference, 396-401, 2011, doi: 10.1109/ACC.2011.5990762.
15. Malan, S.A., and Ventura, L., "A systematic procedure for engine air-path identification", International Journal of Mechanics and Control, vol. 21, no. 1, pp. 127-138, June 2020.
16. Catania, A., Finesso, R., and Spessa, E., "Real-Time Calculation of EGR Rate and Intake Charge Oxygen Concentration for Misfire Detection in Diesel Engines", SAE Technical Paper 2011-24-0149, 2011, doi:10.4271/2011-24-0149.
17. Haykin, S. O., "Neural Networks and Learning Machines", 3rd edition, 2011, Pearson Education, ISBN 0133002551, 9780133002553.
18. Ljung, L., "System identification: theory for the user", 2nd edition, 1999, Upper Saddle River, NJ; Prentice Hall PTR.
19. Nelles, O., "Nonlinear System Identification: From Classical Approaches to Neural Networks and Fuzzy Models", 2013, Springer Berlin Heidelberg.
20. Nørgaard, M., Poulsen, N., and Ravn, O., "Nnsysid and nnctrl - matlab tools for system identification and control with neural networks", IFAC Proceedings Volumes, 30 (11), 931- 936, IFAC Symposium on System Identification (SYSID'97), Kitakyushu, Fukuoka, Japan, 8-11, July 1997, doi:10.1016/S14746670(17)42966-1.

Contact Information

Loris Ventura
Department of Energy, Politecnico di Torino
c.so Duca degli Abruzzi, 24 – 10129 Torino (Italy)
phone: +39-011-090-4535
loris.ventura@polito.it

Acknowledgments

The authors would like to thank profs. Stefano d'Ambrosio and Roberto Finesso from Energy Department, Politecnico di Torino, for their valuable help in developing and revising this work.

Definitions/Abbreviations

a_1, a_2	Correlation parameters
ARX	Auto-Regressive with eXogenous input model
BMEP	Brake Mean Effective Pressure
DOE	Design of Experiment

ECU	Electronic Control Unit
EGR	Exhaust Gas Recirculation
FPT	Fiat Powertrain Technologies
IMAP	Intake Manifold Pressure
MAF	Mass Air Flow
MVEM	Mean Value Engine Model
$\mathbf{n_b}$, $\mathbf{n_f}$, $\mathbf{n_k}$	signal past samples
NARX	Nonlinear Auto-Regressive with eXogenous input model
$\mathbf{NO_x}$	Nitrogen Oxides
NOE	Nonlinear Output Error model
$\mathbf{O_2}$	Diatomic Oxygen

$\mathbf{\Delta O_2}$	Oxygen variation wrt average value
RMSE	Root Mean Square Error
RPM	Revolution per Minute
t	Time
u	Input – controlled variable
VGT	Variable Geometry Turbine
$\mathbf{X_r}$	EGR rate
y	True ouput
$\hat{\mathbf{y}}$	Predicted output

Greek Symbols

THETA	Vector of weight and biases
LAMBDA	Air-to-fuel ratio
PHI	Regressor